IEEE Access
Multidisciplinary ⋮ Rapid Review ⋮ Open Access Journal

Received 3 August 2023, accepted 20 August 2023, date of publication 23 August 2023, date of current version 30 August 2023.

Digital Object Identifier 10.1109/ACCESS.2023.3307719

RESEARCH ARTICLE

An Additive 3D-Printed Hemispherical Lens With Flower-Shaped Stub Slot Ultra-Wideband Antenna for High-Gain Radiation

NONCHANUTT CHUDPOOTI[1], (Member, IEEE), PATCHADAPORN SANGPET[2], TANAPORN PECHRKOOL[2], NATTAPONG DUANGRIT[3], (Member, IEEE), WANWISA THAIWIROT[2], PRAYOOT AKKARAEKTHALIN[2], (Member, IEEE), AND NUTAPONG SOMJIT[4,5,6], (Senior Member, IEEE)

[1]Department of Industrial Physics and Medical Instrumentation, Faculty of Applied Science, King Mongkut's University of Technology North Bangkok, Bangkok 10800, Thailand
[2]Department of Electrical and Computer Engineering, Faculty of Engineering, King Mongkut's University of Technology North Bangkok, Bangkok 10800, Thailand
[3]Centre of Observatory Operations and Engineering (COOE), Division for Radio Observatories Operations and Engineering (CROE), National Astronomical Research Institute of Thailand (Public Organization), Chiang Mai 50180, Thailand
[4]School of Electronic and Electrical Engineering, University of Leeds, LS2 9JT Leeds, U.K.
[5]Division of Micro and Nanosystems (MST), KTH Royal Institute of Technology, 100 44 Stockholm, Sweden
[6]Department of Electrical Engineering, Faculty of Engineering, Chiang Mai University, Muang, Chiang Mai 50200, Thailand

Corresponding author: Nutapong Somjit (n.somjit@leeds.ac.uk)

This work was supported in part by the National Science, Research and Innovation Fund (NSRF); in part by the King Mongkut's University of Technology North Bangkok under Contract KMUTNB-FF-66-49; in part by the Engineering and Physical Science Research Council under Grant EP/S016813/1; and in part by the Swedish Research Council (VR) under Grant 2021-05842_VR.

ABSTRACT This paper presents a 3D-printed hemispherical lens integrated with a planar ultra-wideband (UWB) antenna. The flower-shaped stub slot UWB antenna is made of 0.8-mm FR-4. The operating frequency of the UWB covers 3.10 GHz – 11.6 GHz with a nominal gain at zero degrees of 1.74 dBi. To enhance the UWB antenna's high-gain radiation, a 3D-printed additive hemispherical lens is designed and fabricated from acrylonitrile butadiene styrene (ABS). The electrical properties, i.e., relative permittivity and loss tangent, of ABS are 2.66, and 0.003, respectively. Four different lens radii (8 mm, 10 mm, 12 mm, and 14 mm) are chosen to investigate the gain of the antenna. In all four cases, the 3D-printed lens is fixed in place in front of the UWB antenna with an optimum gap of 3 mm chosen to reduce the wave reflection between the lens and source antenna. Based on the measurement results, the reflection coefficient, S_{11}, of four conditions still covers the UWB frequency range. The nominal gain at zero-degree values for lens radii of 8 mm, 10 mm, 12 mm, and 14 mm are 3.43 dBi, 4.22 dBi, 4.73 dBi, and 5.18 dBi, respectively. The proposed additive 3D-printed dielectric lens antenna also offers many advantages, i.e., ease of design and assembly, low-cost fabrication, and size reduction for high-gain antennas. Furthermore, the high-gain antenna provides a narrow half power beamwidth, which can be implemented to increase the resolution of the imaging system.

INDEX TERMS UWB antenna, hemispherical dielectric lens, 3D-printred lens antenna.

I. INTRODUCTION

A technique called ultra-wideband (UWB) enables high-bandwidth data transmission over a very broad frequency range. This band can allow the transmission of larger files by enabling UWB signals to carry more data. Additionally, because UWB signals can pass through materials like concrete, wooden walls, and furniture, they are a candidate for indoor applications [1], [2], [3]. The benefits of UWB signals include their long range, immunity to interference from most

The associate editor coordinating the review of this manuscript and approving it for publication was Ali Karami Horestani.

electronic equipment, and ability to simultaneously use multiple transmission frequencies to reach high data speeds. Many researchers have created a variety of UWB antennas based on these characteristics. Despite their widespread usage, the antenna's structure, size, and material composition ultimately determine its efficiency; accordingly, numerous approaches have been investigated and developed to enhance antenna properties [4], [5], [6], [7], [8], [9], [10], [11], [12], [13], [14], [15], [16], [17], [18], [19], [20], [21], [22].

In recent years, most researchers have focused on improving antenna characteristics, e.g., bandwidth, gain, and radiation pattern. The most common methods for enhancing the antenna gain and improving the radiation patterns of UWB antennas include arrays [4], [5], [6], reflectors [7], [8], [9], [10], and metamaterials [5], [11], [12], [13], [14]. While these methods can increase the gain and improve radiation patterns, they also make the antenna larger and more complex. Using a lens integrated with the antenna is a promising approach that has been presented in numerous studies [15], [16], [17], [18], [19], [20], [21], [22]. Although this is not a new technique, it has often been used to increase the gain and radiation characteristics of UWB antennas.

A dielectric lens mounted on a planar antenna can be fabricated using the micro-machining process; however, the micro-machining process involves many fabrication steps and hence is expensive. As an alternative, 3D-printing technology is receiving considerable attention in the fabrication of lenses for planar antennas.

The 3D-printed lens is an alternative technique to enhance antenna gain and improve antenna performance by reducing the complexity of the fabrication process. Various shapes of dielectric lenses have been investigated [16], [17], [23], [24], [25], [26], [27], [28], [29]. In [23] and [25], the grin lens was designed to be placed on top of the antenna source, and the number of layers of the grin lens was used to control the antenna gain. Hemispherical lenses [29], and conical lenses [16] were designed based on the elliptical shape to conform the radiation pattern in the UWB range. The advantages of 3D-printing techniques include ease of fabrication, rapid prototyping capability, and low cost [18], [22], [30], [31]. Additionally, 3D printing techniques allow the use of a variety of conductor and dielectric materials.

This paper presents an additive 3D-printed lens embedded with a UWB antenna. The structure of the UWB antenna is designed from a flower-shaped stub slot, which is made of a conventional epoxy substrate (FR-4) with a thickness of 0.8 mm. The measured nominal gain of the UWB antenna is 1.74 dBi at zero degrees. The structure of the 3D-printed dielectric lens antenna is hemispherical; the ratio of the lens radius and extended lens configuration is discussed in [20]. The electrical properties of the acrylonitrile butadiene styrene (ABS) material, which is used for fabrication, were investigated using the Keysight 85072A 10-GHz split cylinder resonator method [32]. The relative permittivity and loss tangent values of ABS are 2.66 and 0.003, respectively. Four

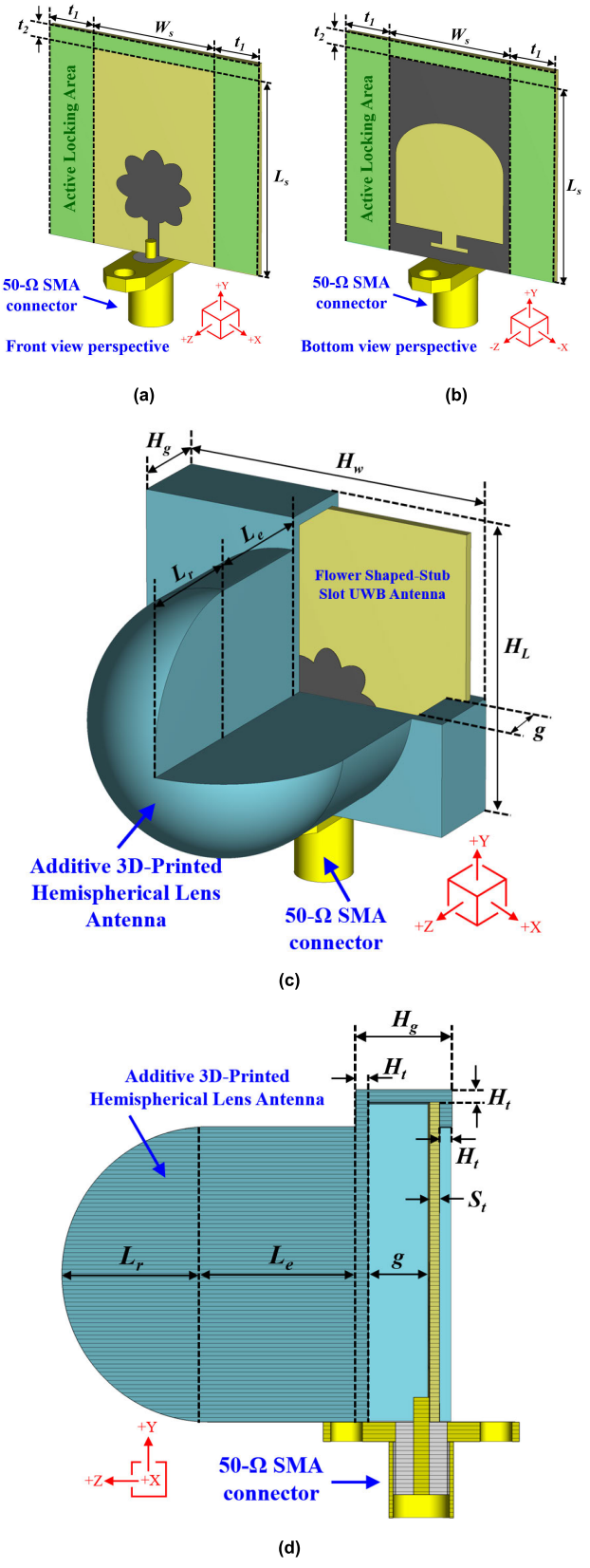

FIGURE 1. The geometry of the flower-shaped stub slot UWB antenna: (a) front view perspective, (b) back view perspective, (c) perspective view after embedding the hemispherical lens, and (d) cross-section view after embedding the hemispherical lens.

lens radius values (8 mm, 10 mm, 12 mm, and 14 mm) are chosen to investigate the antenna characteristics, i.e., the reflection coefficient, gain, radiation pattern, and half power beamwidth (HPBW). Based on the measurement results, the reflection coefficient, S_{11}, of the four studied conditions still covers the UWB frequency range, with values of 3.10 GHz to 11.60 GHz. The nominal gain at zero-degree for the four lens radii of 8 mm, 10 mm, 12 mm, and 14 mm increased to 3.43 dBi, 4.22 dBi, 4.73 dBi, and 5.18 dBi, respectively. At 7 GHz, which represents the center of the UWB range, the HPBW values for the lens radii of 8 mm, 10 mm, 12 mm, and 14 mm are 121.1 degrees, 89.2 degrees, 73.4 degrees, and 59.9 degrees, respectively.

II. UWB ANTENNA AND 3D-PRINTED LENS DESIGN

A. FLOWER SHAPED-STUB SLOT UWB ANTENNA

The geometry of the front and bottom perspective views of the flower-shaped stub slot antenna are shown in Figures 1(a) and 1(b), respectively. The antenna is designed in a flower-shaped stub in front view, and its back view is designed with an inverted T-shaped slot and an inverted U-shaped slot, which are etched on the ground plane. This flower-shaped antenna was previously studied in [33], in which it was made using an FR-4 substrate and operated at a frequency range of 3.1 GHz – 12.5 GHz corresponding to a relative permittivity, ε_r, of 4.3 and a loss tangent, $tan\delta$, of 0.025. The dimensions of the UWB antenna in [23] were a width, W_s, of 16 mm, a length, L_S, of 24 mm, and a substrate thickness, S_t, of 0.8 mm. The average antenna gain at zero-degree was 1.74 dBi. The radiation pattern in the xz-plane is nearly omnidirectional at low frequency and bi-directional at high frequency. Based on the above, the flower-shaped antenna has low gain. At high frequencies, the beam is not situated in the center of the antenna and its direction cannot be controlled. Accordingly, a hemispherical lens was selected in this study and incorporated with the flower-shaped stub slot antenna to achieve a configurable beam and increase the antenna gain by increasing the lens radius. However, the previous size of the flower-shaped stub slot antenna cannot connect with the 3D-printed dielectric lens antenna due to its smaller active area. Therefore, the authors of the present study modified the UWB antenna by adding an active locking area (t_1 and t_2), as shown by the green region in Figures 1(a) and 1(b). The length values of t_1 and t_2 are 6 mm and 2 mm, respectively. The final modified UWB antenna has a width of 28 mm and a length of 26 mm.

B. 3D-PRINTED HEMISPHERICAL LENS DESIGN

A 3D-printed hemispherical lens design [20] was selected to enhance antenna performance, i.e., the antenna gain, HPBW, and radiation pattern. Figures 1(c) and 1(d) depict the 3D geometry and a cross-section view of the hemispherical lens, respectively. The hemispherical lens comprises three key sections. The first section is the lens radius, L_r, which is chosen to enhance the antenna's gain. The second section is the lens extension length, L_e, which is used to decrease the overall incidence of the side lobe of the antenna radiation pattern. To determine L_r and L_e, the ratio of these quantities is fixed at 1 to achieve the maximum realized gain at zero degrees [20]. The third section is the housing section, which is used for the locking lens UWB antenna with a flower-shaped stub slot. The key parameters of the designed 3D-printed hemispherical lens are listed in Table 1.

TABLE 1. The parameters of the 3D-printed hemispherical lens with flower-shaped stub slot ultra-wideband antenna.

Parameters	Explanation	Values (mm.
W_s	Width of the flower-shaped antenna	16
L_s	Length of the flower-shaped antenna	24
t_1	Length of the active locking area at side of the antenna	6
t_2	Length of the active locking area on top of the antenna	2
L_r	Hemispherical lens radius	8, 10, 12, 14
L_e	Hemispherical lens extension length	8, 10, 12, 14
H_w	Width of housing	30
H_L	Length of housing	27
H_g	Thickness of housing	5.8
H_t	Thickness of stopper substrate	1
g	Gap between hemispherical lens and the UWB antenna	3

The hemispherical lens is made of ABS, an engineering plastic widely used in many industries due to its excellent mechanical properties. It is a versatile material capable of withstanding high-impact forces and high temperatures, thus making it suitable for printing both functional prototypes and end-use parts. To characterize the electrical properties, i.e., ε_r and $tan\delta$, of the 3D-printed ABS material, the Keysight 85072A 10-GHz split cylinder resonator method [32] was chosen. The size of the analyzed sample was 60 mm × 60 mm with a thickness of 2 mm; this sample was printed with an infill density of 95%. The 3D printer used in this study is a Zortrax M200 [34]. The measured values of ε_r and $tan\delta$ at 10 GHz for the ABS used in this study were 2.66 and 0.003, respectively.

The hemispherical lens was designed with four L_r values from 8 to 14 mm in steps of 2 mm, and the efficiency of the antenna gain and the radiation pattern for each configuration were simulated. Table 2 shows the comparison of the total antenna efficiency without and with four lens radii, L_r. The optimized gap, g, between the flower-shaped stub slot UWB antenna and the 3D-printed hemispherical lens is set to 3 mm, which was simulated using the 3D EM simulation tool CST Studio Suite [35]. The simulated reflection coefficient was determined both with and without a hemispherical lens, as illustrated in Figure 2(a). The simulated results show that the antenna without a lens has a frequency range of 3.06 GHz –11.48 GHz when calculated at a reflection coefficient below -10 dB. The antennas with dielectric lenses of 8 mm, 10 mm,

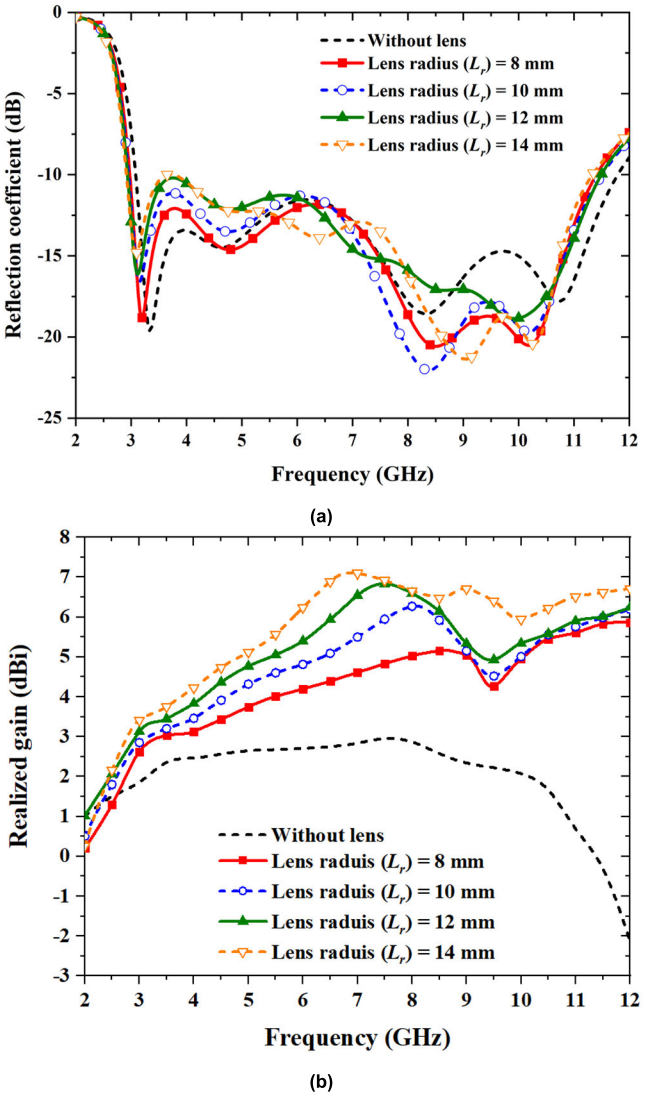

FIGURE 2. The simulated results of the (a) reflection coefficient, S_{11}, and (b) realized gain at zero degrees for both the antenna without a lens and with the four lens radii of 8, 10, 12, and 14 mm.

TABLE 2. A comparison between the total antenna efficiency of with and without a 3D-printed hemispherical lens antenna.

Lens radius, L_r, (mm)	Total antenna efficiency (%)		
	3.5 GHz	7 GHz	10 GHz
Without Lens	89.04	80.88	15.49
8 mm	90.18	89.08	81.73
10 mm	92.24	90.36	83.40
12 mm	92.47	91.94	87.27
14 mm	93.95	92.83	87.69

12 mm, and 14 mm size have operating frequency ranges of 2.97 GHz – 11.37 GHz, 2.96 GHz – 11.41 GHz, 2.99 GHz – 12 GHz, and 2.90 GHz – 11.45 GHz, respectively.

Figure 2(b) shows the simulated realized gain of the antenna with and without the four studied lenses. The average

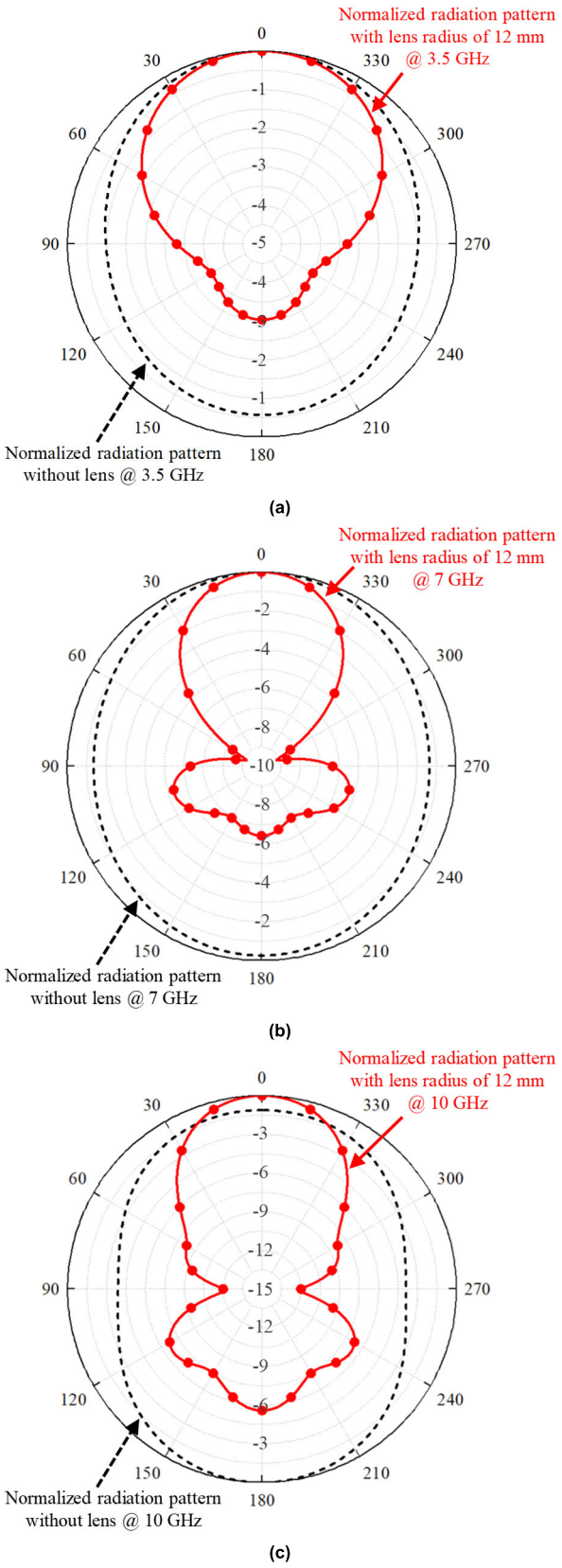

FIGURE 3. Comparison between the normalized radiation patterns with and without 3D-printed lens antenna at (a) 3.5 GHz, (b) 7 GHz, and (c) 10 GHz. The lens radius and lens extension length are both fixed at 12 mm.

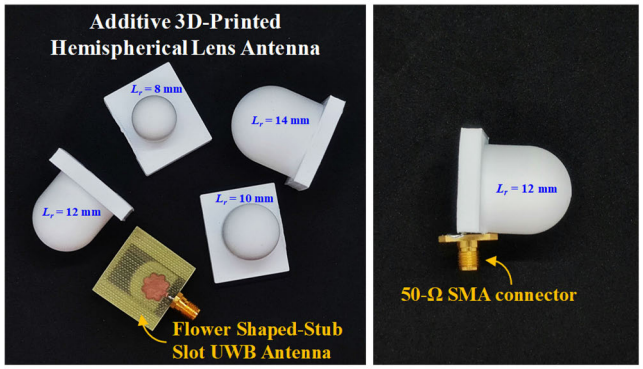

FIGURE 4. The fabricated flower-shaped stub slot UWB antenna with different four 3D-printed hemispherical lens antennas (a) before assembly and (b) after assembly.

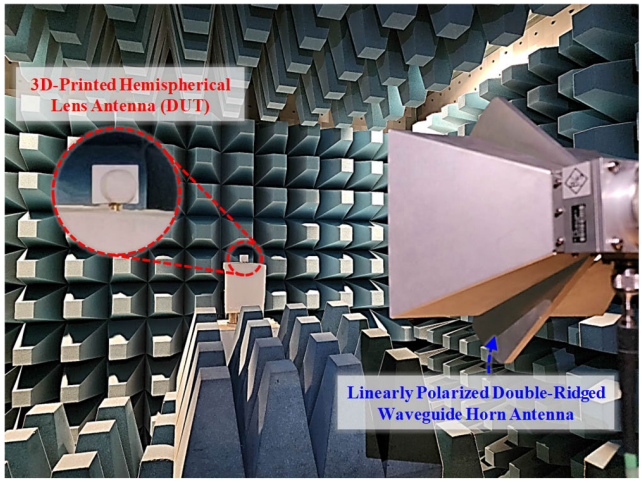

FIGURE 5. Measurement setup in an anechoic chamber. The fabricated 3D-printed lens antenna is placed on a turntable. A linearly polarized double-ridged wave horn antenna, which is a standard antenna, is used for the radiation pattern and antenna gain measurement.

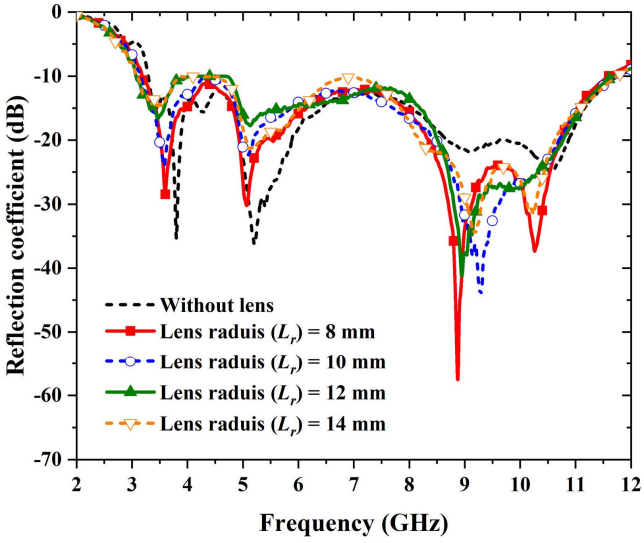

FIGURE 6. The measured reflection coefficient, S_{11}, of the antenna without a lens and with the four studied lens radii (8 mm, 10 mm, 12 mm, and 14 mm).

gain at zero degrees of the antenna without a 3D-printed lens antenna is 1.77 dBi, whereas the average gain values for the 3D-printed lens antennas of 8 mm, 10 mm, 12 mm, and 14 mm are 4.65 dBi, 5.26 dBi, 5.77 dBi, and 6.56 dBi, respectively. Based on the simulated results for lens radii of 8 mm to 14 mm, the antenna gain at zero degrees will increase with increasing lens radius.

Figure 3 shows a comparison between the simulated results of the 2D-normalized radiation pattern of the flower-shaped stub slot UWB antenna both with and without a hemispherical lens by fixing the lens radius at 12 mm. Three frequencies (3.5 GHz, 7 GHz, and 10 GHz) were selected to compare the low-, middle-, and high-frequency performance of the UWB antenna. Based on the simulated results, for the flower-shaped stub slot UWB antenna only, the antenna's radiation pattern is bi-directional. In contrast, when the 3D-printed hemispherical lens antenna is integrated, the radiation patterns are changed to directional. Thus, these results indicate that the 3D-printed lens antenna can reconfigure the radiating beam from a bi-directional to a directional beam antenna.

C. FABRICATION AND ASSEMBLY

The completed models of the proposed flower-shaped antenna were exported from the simulation tool, CST Microwave Studio Suite, using the DXF file format. The top view and bottom view of the antenna were routed and fabricated using an LPKF ProtoMat S100 circuit board plotter [36], which has a high travel speed of up to 50 mm/sec and a cutting resolution of 0.25 μm. When finishing with circuit board plotter, the fabricated prototype of a flower-shaped antenna connecting with a 50-ohm SMA Panel Jack 2-Hole Flange Straight Flat Tab WR-SMA [37].

The Zortrax M200, a fused deposition modeling machine, was used to fabricate the hemispherical lens used in this study. The proposed lens antenna was constructed from ABS with a filament diameter of 1.75 mm. The 3D EM simulation program CST Studio's STL file format was used to export the final 3D models of the proposed hemispherical lens. For printing, the layer printing thickness was set to 90 μm using a nozzle diameter of 0.4 mm and a 95% infill density. Figure 4 shows the fabricated prototype of the flower-shaped stub slot UBW antenna with the four different 3D-printed hemispherical lens radii.

III. MEASUREMENT SETUP AND RESULTS

A. MEASUREMENT SETUP

A Rohde & Schwarz ZVB-20 vector network analyzer (VNA) was used to measure the reflection coefficient, S_{11}, and radiation pattern of the four fabricated hemispherical lens antennas. To measure S_{11}, the Through-Open-Short-Match (TOSM) calibration method was selected. The start and stop frequency values were set to 3.0 GHz and 12 GHz,

TABLE 3. A comparison between the half power beamwidth (HPBW) with and without a 3D-printed hemispherical lens antenna.

Lens radius, L_r, (mm)	3.5 GHz (degree)	7 GHz (degree)	10 GHz (degree)
Without Lens	104	155	109
8 mm	104	139	104
10 mm	103	100	80
12 mm	100	67	56
14 mm	98	53	47

respectively. The number of points was set to 901. To measure the radiation pattern of the proposed lens antenna, a linearly polarized R&S®HF907 double-ridged wave horn antenna [38] was used as a reference antenna. The frequency range of the standard horn is 800 MHz to 18 GHz. A DAMs Heavy-Duty Antenna Model-5100 turntable was used to rotate the device under test (DUT); this was connected with the VNA and controlled using Diamond Studio Antenna Measurement Studio Software [39]. The distance between the reference antenna and the DUT was set from a far-field condition. The turntable was automatically rotated from 0° to 360° in steps of 1°. Figure 5 shows the measurement setup of the 3D-printed lens antenna and a standard antenna in an anechoic chamber.

B. MEASUREMENT RESULTS

The reflection coefficients, S_{11}, for the flower-shaped antenna with all four hemispherical lens sizes are shown in Figure 6. Based on the measured results, the lens radius, L_r, of the hemispherical lens at 8 mm, 10 mm, 12 mm, and 14 mm can cover the UWB frequency range, when calculating the reflection coefficient, S_{11}, lower than -10 dB. The reflection coefficient values, S_{11}, corresponding to dielectric lens radii of 8 mm, 10 mm, 12 mm, and 14 mm are 3.10 GHz – 11.58 GHz, 3.08 GHz – 11.76 GHz, 3.08 GHz – 11.68 GHz, and 3.05 GHz – 11.74 GHz, respectively.

The measured radiation patterns are shown in Figure 7. The three sampling frequencies of 3.5 GHz, 7 GHz, and 10 GHz were selected to represent the low, middle, and high frequencies of the UWB range. To clearly visualize the enhancement antenna gain, the normalized condition was calculated for only the flower-shaped stub slot UWB antenna. At a zero-degree angle and a low frequency of 3.5 GHz, increasing lens radii of 8 mm, 10 mm, 12 mm, and 14 mm correspond to gain increases to +0.14 dBi, +0.47 dBi, +0.50 dBi, and +1.06 dBi, respectively, as shown in Figure 7(a). At an intermediate frequency of 7 GHz, Figure 7(b) shows that the antenna gain increased to +1.87 dBi, +2.96 dBi, +4.57 dBi, and +4.77 dBi for lens radii of 8, 10, 12, and 14 mm, respectively. Finally, for the high-frequency 10 GHz band, the antenna gain values for increasing lens radius increased to +1.89 dBi, +2.73 dBi, +5.12 dBi, and +5.33 dBi, as shown in Figure 7(c). Based on the measured radiation pattern results

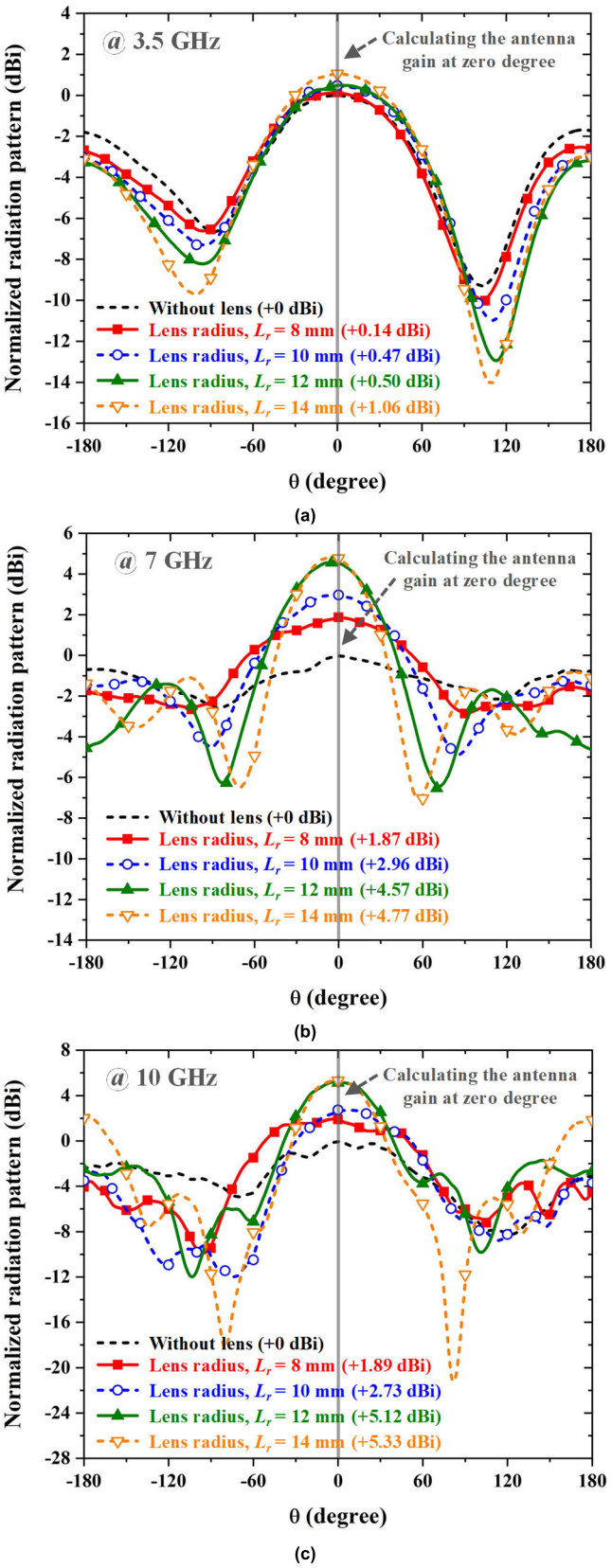

FIGURE 7. The radiation patterns of the four 3D-printed dielectric lens antennas (8, 10, 12, and 14 mm) compared with the antenna without a dielectric lens measured at (a) 3.5 GHz, (b) 7 GHz, and (c) 10 GHz.

TABLE 4. A comparison key factor of the lens design of this work and other published works.

References	Lens Material	Lens structure	Lens fabrication process	Plug & play lens function	Frequency (GHz)	Overall dimension (mm^3) (λ_L = lowest wavelength of the operating frequency)	Maximum gain increment (dBi)
[23]	Rogers RO4003	GRIN lens	Milling machine	Yes	3.4 – 11.0	1.93 λ_L ×1.42 λ_L × 1.13 λ_L	5.3 @ 8.8 GHz
[24]	Rogers RO4003C	Half elliptical-shaped dielectric lens (HEDL)	Milling machine	No	1.0 – 30.0	0.32 λ_L × 0.46 λ_L × 0.00169 λ_L	N/A
[25]	Rogers RO4003C	GRIN lens	Milling machine	Yes	0.84 – 13.0	0.14 λ_L × 0.6 λ_L × 0.78 λ_L	7.73 @ 9.5 GHz
[26]	Flexible polyimide	Phase adjusting unit (PAU) lens	Milling and bending the flexible PAU dynamically	Yes	6.0 – 18.0	N/A	2.2 @ 15.4 GHz
[27]	Rogers Arlon Iso 917	Metasurface lens	Milling machine	No	1.0 – 6.0	N/A	4.8 @ 5.5 GHz
[28]	Teflon (PTFE)	Spherical–axicon dielectric lens	3D printing technology	Yes	0.65 – 6.0	0.43 λ_L × 0.43 λ_L × 0.73 λ_L	6.3 @ 6 GHz
[29]	ECCOSTOCK HIK 500F	Hemispherical lens	3D printing technology	Yes	4.0 – 12.0	1.27 λ_L × 1.27 λ_L × 1.67 λ_L	N/A
[16]	High-density polyethylene	Conical frustum lens	3D printing technology	Yes	20.5– 40.0	1.64 λ_L × 1.64 λ_L × 1.71 λ_L	N/A
[17]	Photo-curable plastic resin	Comb mushroom-like lens	3D printing technology	Yes	14.0 – 20.0	1.1 λ_L × 2.24 λ_L × 0.56 λ_L	4.7
This work	**Acrylonitrile butadiene styrene (ABS)**	**Hemispherical lens**	**3D printing technology**	**Yes**	**3.10 – 11.58**	**Lens radius = 8.0 mm 0.31 λ_L × 0.28 λ_L× 0.27 λ_L**	**3.43 @ 9 GHz**
					3.08 – 11.76	**Lens radius = 10.0 mm 0.31 λ_L × 0.28 λ_L× 0.29 λ_L**	**4.22 @ 9 GHz**
					3.08 – 11.68	**Lens radius = 12.0 mm 0.31 λ_L × 0.28 λ_L× 0.31 λ_L**	**4.73 @ 9 GHz**
					3.05 – 11.74	**Lens radius = 14.0 mm 0.31 λ_L × 0.28 λ_L × 0.34 λ_L**	**5.18 @ 9 GHz**

for a zero-degree angle, combining the hemispherical lens and flower-shaped antenna achieves high gain and reconfigures the radiation beam from bidirectional to marginally unidirectional, depending on the radius of the hemispherical lens.

Table 3 summarizes the results of the measured HPBW for the four fabricated lens antennas, compared with the bare flower-shaped stub slot UWB antenna. At a low frequency of 3.5 GHz, the HPBW slightly decreases with increasing lens radius. However, at the middle frequency of 7 GHz and high frequency of 10 GHz, the HPBW rapidly drops from 155 degrees to 53 degrees and from 109 degrees to 47 degrees, respectively. Thus, this narrow HPBW could be potentially applied in many applications, including increasing antenna resolution or detecting small objects.

IV. CONCLUSION AND FUTURE WORK

This study proposed an ultra-wideband antenna with a flower-shaped stub combined with a 3D-printed hemispherical lens. The UWB antenna has a width of 28 mm, a length of 26 mm, and a thickness of 0.8 mm and was assembled with a dielectric hemispherical lens. Four lens radii of 8 mm, 10 mm, 12 mm, and 14 mm, were chosen to investigate the antenna's characteristics. Based on the measured results, the reflection coefficient, S_{11}, of the antenna with and without a dielectric lens can cover the operating frequency of UWB (3.1 GHz – 10.6 GHz). The antenna gain at zero degrees will increase with increasing lens radius. Table 4 extensively shows the figure-of-merit comparisons of the lens processes with other published works, [16], [17] and [23], [24], [25], [26], [27], [28], [29]. This technique provides many advantages, including ease of design, low complexity of fabrication and plug & play function, enhancing the antenna gain, and providing reconfigurable beams; thus, the proposed technique can be applied to improve the resolution of various imaging applications.

REFERENCES

[1] Z.-Y. Zhang, G. Fu, W.-J. Wu, J. Lei, and S.-X. Gong, "A wideband dual-sleeve monopole antenna for indoor base station application," *IEEE Antennas Wireless Propag. Lett.*, vol. 10, pp. 45–48, 2011, doi: 10.1109/LAWP.2011.2108255.

[2] Y. Qi, B. Yuan, Y. Cao, and G. Wang, "An ultrawideband low-profile high-efficiency indoor antenna," *IEEE Antennas Wireless Propag. Lett.*, vol. 19, no. 2, pp. 346–349, Feb. 2020, doi: 10.1109/LAWP.2019.2962265.

[3] B. Q. Wu and K.-M. Luk, "A wideband, low-profile, conical-beam antenna with horizontal polarization for indoor wireless communications," *IEEE Antennas Wireless Propag. Lett.*, vol. 8, pp. 634–636, 2009, doi: 10.1109/LAWP.2009.2023545.

[4] R. Lian, Z. Wang, Y. Yin, J. Wu, and X. Song, "Design of a low-profile dual-polarized stepped slot antenna array for base station," *IEEE Antennas Wireless Propag. Lett.*, vol. 15, pp. 362–365, 2016, doi: 10.1109/LAWP.2015.2446193.

[5] F.-M. Yang, L. Peng, X. Liao, K.-S. Mo, X. Jiang, and S.-M. Li, "Coupling reduction for a wideband circularly polarized conformal array antenna with a single-negative structure," *IEEE Antennas Wireless Propag. Lett.*, vol. 18, no. 5, pp. 991–995, 2019, doi: 10.1109/LAWP.2019.2907134.

[6] D. Sipal, M. P. Abegaonkar, and S. K. Koul, "Easily extendable compact planar UWB MIMO antenna array," *IEEE Antennas Wireless Propag. Lett.*, vol. 16, pp. 2328–2331, 2017, doi: 10.1109/LAWP.2017.2717496.

[7] P. Singsura, T. Hongnara, W. Thaiwirot, and P. Akkaraekthalin, "Design of antenna reflector using two layer frequency selective surfaces for directivity enhancement in UWB application," in *Proc. Int. Symp. Antennas Propag. (ISAP)*, Oct. 2017, pp. 1–2, doi: 10.1109/ISANP.2017.8228982.

[8] R. A. Penchel, S. R. Zang, J. R. Bergmann, and F. J. S. Moreira, "Design of wideband omnidirectional dual-reflector antennas in millimeter waves," *IEEE Antennas Wireless Propag. Lett.*, vol. 18, no. 5, pp. 906–910, May 2019, doi: 10.1109/LAWP.2019.2905602.

[9] T. Sutham, W. Thaiwirot, and P. Akkaraekthalin, "Design of ultra-wideband inverted U-shaped slot antenna with reflector for GPR applications," in *Proc. 19th Int. Conf. Electr. Eng./Electron., Comput., Telecommun. Inf. Technol. (ECTI-CON)*, May 2022, pp. 1–4, doi: 10.1109/ECTI-CON54298.2022.9795528.

[10] K. Phaebua, N. Chudpooti, S. Kittiwittayapong, T. Lertwiriyaprapa, D. Torrungrueng, and H.-T. Chou, "One-sixteenth spherical homogeneous dielectric lens antenna using partially reflective surface for size reduction and high-gain radiation," *IEEE Antennas Wireless Propag. Lett.*, vol. 20, no. 2, pp. 184–188, Feb. 2021, doi: 10.1109/LAWP.2020.3043629.

[11] X. Li, H. Zhou, Z. Gao, H. Wang, and G. Lv, "Metamaterial slabs covered UWB antipodal Vivaldi antenna," *IEEE Antennas Wireless Propag. Lett.*, vol. 16, pp. 2943–2946, 2017, doi: 10.1109/LAWP.2017.2754860.

[12] T. Shabbir, R. Saleem, S. S. Al-Bawri, M. F. Shafique, and M. T. Islam, "Eight-port metamaterial loaded UWB-MIMO antenna system for 3D system-in-package applications," *IEEE Access*, vol. 8, pp. 106982–106992, 2020, doi: 10.1109/ACCESS.2020.3000134.

[13] X. Shi, Y. Cao, Y. Hu, X. Luo, H. Yang, and L. H. Ye, "A high-gain antipodal Vivaldi antenna with director and metamaterial at 1–28 GHz," *IEEE Antennas Wireless Propag. Lett.*, vol. 20, no. 12, pp. 2432–2436, Dec. 2021, doi: 10.1109/LAWP.2021.3114061.

[14] J. Ha, K. Kwon, Y. Lee, and J. Choi, "Hybrid mode wideband patch antenna loaded with a planar metamaterial unit cell," *IEEE Trans. Antennas Propag.*, vol. 60, no. 2, pp. 1143–1147, Feb. 2012, doi: 10.1109/TAP.2011.2173114.

[15] N. Chudpooti, P. Sangpet, N. Duangrit, P. Akkaraekthalin, I. D. Robertson, and N. Somjit, "An integrated 3D-printed lens with ultra-wideband flower-shaped stub antenna for ethanol-water mixture characterization," in *Proc. Res., Invention, Innov. Congr., Innov. Electricals Electron. (RI2C)*, Sep. 2021, pp. 80–83, doi: 10.1109/RI2C51727.2021.9559770.

[16] G. H. Lee, S. Kumar, H. C. Choi, and K. W. Kim, "Wideband high-gain double-sided dielectric lens integrated with a dual-bowtie antenna," *IEEE Antennas Wireless Propag. Lett.*, vol. 20, no. 3, pp. 293–297, Mar. 2021, doi: 10.1109/LAWP.2020.3048165.

[17] Y.-X. Zhang, Y.-C. Jiao, and S.-B. Liu, "3-D-printed comb mushroom-like dielectric lens for stable gain enhancement of printed log-periodic dipole array," *IEEE Antennas Wireless Propag. Lett.*, vol. 17, no. 11, pp. 2099–2103, Nov. 2018, doi: 10.1109/LAWP.2018.2851298.

[18] M. F. Farooqui and A. Shamim, "3-D inkjet-printed helical antenna with integrated lens," *IEEE Antennas Wireless Propag. Lett.*, vol. 16, pp. 800–803, 2017, doi: 10.1109/LAWP.2016.2604497.

[19] G. Savvides, N. Duangrit, N. Chudpooti, P. Akkaraekthalin, U. Imberg, I. D. Robertson, and N. Somjit, "3D rapid-prototyped 21–31-GHz hollow SIWs for low-cost 5G IoT and robotic applications," *IEEE Access*, vol. 9, pp. 11750–11760, 2021, doi: 10.1109/ACCESS.2021.3051180.

[20] N. Chudpooti, N. Duangrit, P. Akkaraekthalin, I. D. Robertson, and N. Somjit, "220–320 GHz hemispherical lens antennas using digital light processed photopolymers," *IEEE Access*, vol. 7, pp. 12283–12290, 2019, doi: 10.1109/ACCESS.2019.2893230.

[21] N. Chudpooti, S. Praesomboon, N. Duangrit, N. Somjit, and P. Akkaraekthalin, "An X-band portable 3D-printed lens antenna with integrated waveguide feed for microwave imaging," in *Proc. Photon. Electromagn. Res. Symp.*, Rome, Italy, Jun. 2019, pp. 487–492, doi: 10.1109/PIERS-Spring46901.2019.9017614.

[22] N. Chudpooti, N. Duangrit, P. Akkaraekthalin, I. D. Robertson, and N. Somjit, "Electronics-based free-space terahertz measurement using hemispherical lens antennas," *IEEE Access*, vol. 7, pp. 95536–95546, 2019, doi: 10.1109/ACCESS.2019.2929697.

[23] R. Singha and D. Vakula, "Directive beam of the monopole antenna using broadband gradient refractive index metamaterial for ultra-wideband application," *IEEE Access*, vol. 5, pp. 9757–9763, 2017, doi: 10.1109/ACCESS.2017.2703876.

[24] M. Moosazadeh, S. Kharkovsky, J. T. Case, and B. Samali, "Miniaturized UWB antipodal Vivaldi antenna and its application for detection of void inside concrete specimens," *IEEE Antennas Wireless Propag. Lett.*, vol. 16, pp. 1317–1320, 2017.

[25] Z. Yang, L. Guo, C. Yao, Q. Zhang, Z. Xu, M. Guo, and Z. Wang, "Ultrawideband antipodal tapered slot antenna with gradient refractive index metamaterial lens," *IEEE Antennas Wireless Propag. Lett.*, vol. 18, no. 12, pp. 2741–2745, Dec. 2019.

[26] L. Sang, S. Wu, G. Liu, J. Wang, and W. Huang, "High-gain UWB Vivaldi antenna loaded with reconfigurable 3-D phase adjusting unit lens," *IEEE Antennas Wireless Propag. Lett.*, vol. 19, no. 2, pp. 322–326, Feb. 2020.

[27] O. Yesilyurt and G. Turhan-Sayan, "Metasurface lens for ultra-wideband planar antenna," *IEEE Trans. Antennas Propag.*, vol. 68, no. 2, pp. 719–726, Feb. 2020.

[28] R. Cicchetti, V. Cicchetti, A. Faraone, L. Foged, and O. Testa, "A compact high-gain wideband lens Vivaldi antenna for wireless communications and through-the-wall imaging," *IEEE Trans. Antennas Propag.*, vol. 69, no. 6, pp. 3177–3192, Jun. 2021.

[29] O. Yurduseven, D. Cavallo, and A. Neto, "Wideband dielectric lens antenna with stable radiation patterns fed by coherent array of connected leaky slots," *IEEE Trans. Antennas Propag.*, vol. 62, no. 4, pp. 1895–1902, Apr. 2014.

[30] B. Hong, M. Swithenbank, N. Greenall, R. G. Clarke, N. Chudpooti, P. Akkaraekthalin, N. Somjit, J. E. Cunningham, and I. D. Robertson, "Low-loss asymptotically single-mode THz Bragg fiber fabricated by digital light processing rapid prototyping," *IEEE Trans. THz Sci. Technol.*, vol. 8, no. 1, pp. 90–99, Jan. 2018, doi: 10.1109/TTHZ.2017.2778047.

[31] N. Chudpooti, G. Savvides, N. Duangrit, P. Akkaraekthalin, I. D. Robertson, and N. Somjit, "Harmonized rapid prototyping of millimeter-wave components using additive and subtractive manufacturing," *IEEE Trans. Compon., Packag., Manuf. Technol.*, vol. 12, no. 7, pp. 1241–1248, Jul. 2022, doi: 10.1109/TCPMT.2022.3181886.

[32] Keysight. *Specification and Operational Characteristics of Keysight 85072A 10-GHz Split Cylinder Resonator*. Accessed: May 6, 2022. [Online]. Available: https://www.keysight.com/us/en/assets/7018-01496/technical-overviews/5989-6182

[33] P. Sangpet, W. Thaiwirot, and P. Akkaraekthalin, "A compact microstrip-fed slot antenna with flower-shaped stub for ultra-wideband applications," in *Proc. Int. Electr. Eng. Congr. (iEECON)*, Mar. 2017, pp. 1–4, doi: 10.1109/IEECON.2017.8075840.

[34] Zortrax. *Specification and Operational Characteristics of Zortrax M Series 3D Printer*. Accessed: Jul. 12, 2022. [Online]. Available: https://support.zortrax.com/m-series-specification/

[35] *CST-MW Studio*, Comput. Simul. Technol., Framingham, MA, USA, 2017.

[36] LPKF. *Specification and Operational Characteristics of LPKF ProtoMat S100*. Accessed: Jan. 8, 2022. [Online]. Available: http://www.spezial.cz/pdf/protomat_s100.pdf

[37] WURTH ELEKTRPNIK. *Specification and Operational Characteristics of SMA Panel Jack 2-Hole Flange Straight Flat Tab WR-SMA*. Accessed: Jan. 20, 2022. [Online]. Available: https://www.we-online.com/en/components/products/WR-SMA_60312312114616

[38] Rohde & Schwarz. *R&S?HF907 Double-Ridged Waveguide Horn Antenna*. Accessed: Sep. 12, 2022. [Online]. Available: https://scdn.rohde-schwarz.com/ur/pws/dl_downloads/dl_common_library/dl_brochures_and_datasheets/pdf_1/HF907_2020.pdf

[39] Diamond Engineering. *Antenna Measurement Software*. Accessed: Mar. 19, 2022. [Online]. Available: http://www.diamondeng.net/PDF/software specs.pdf

NONCHANUTT CHUDPOOTI (Member, IEEE) received the B.Sc. degree (Hons.) in industrial physics and medical instrumentation and the Ph.D. degree in electrical engineering from the King Mongkut's University of Technology North Bangkok, Bangkok, Thailand, in 2012 and 2018, respectively.

He was appointed as a Lecturer with the Department of Industrial Physics and Medical Instrumentation, Faculty of Applied Science, in 2018. His research interests include the application of microwave microfluidic sensors, millimeter-wave substrate integrated circuit applications, and substrate integrated waveguide applications.

Dr. Chudpooti was a recipient of the Best Presentation Award from the Thailand–Japan Microwave, in 2015 and 2018, and the Young Researcher Encouragement Award, in 2016.

PATCHADAPORN SANGPET was born in Chiang Rai, Thailand, in 1992. She received the bachelor's degree in industrial physics and medical equipment and the master's degree in electrical and computer engineering from the King Mongkut's University of Technology North Bangkok (KMUTNB), Bangkok, Thailand, in 2013 and 2016, respectively, where she is currently pursuing the Ph.D. degree with the Department of Electrical and Computer Engineering. Her research interests include ultra-wideband antenna, microwave sensor, and 3D-printed for application.

TANAPORN PECHRKOOL was born in Chumphon, Thailand, in 1987. He received the B.Eng. degree in electronics and telecommunications engineering from the Rajamangala University of Technology Phra Nakhon, in 2010, and the M.Eng. degree in electrical engineering from the King Mongkut's University of Technology North Bangkok (KMUTNB), Thailand, in 2014. He is currently pursuing the Ph.D. degree with the Department of Electrical and Computer Engineering. He is also a Lecturer with the Faculty of Engineering, Rajamangala University of Technology Thanyaburi. His research interests include microwave sensor, ZOR antenna, and telecommunication.

NATTAPONG DUANGRIT (Member, IEEE) received the B.Eng. degree in electronics and telecommunication engineering from the Rajamangala University of Technology Thanyaburi (RMUTT), Chiang Mai, Thailand, in 2014, and the Ph.D. degree from the King Mongkut's University of Technology North Bangkok (KMUTNB), Bangkok, Thailand, in 2019. His current research interests include the application of 3-D printing technology for millimeter-wave and THz devices and substrate integrated waveguide applications. He received the Thailand Research Fund through the Royal Golden Jubilee Ph.D. Program for his Ph.D. degree.

WANWISA THAIWIROT received the B.Eng., M.Eng., and D.Eng. degrees in telecommunication engineering from the Suranaree University of Technology (SUT), Nakhon Ratchasima, Thailand, in 2003, 2007, and 2011, respectively. In 2012, she joined the Department of Electrical Engineering, King Mongkut's University of Technology North Bangkok (KMUTNB). Her current research interests include wideband and ultra-wideband antennas, and microwave applications.

PRAYOOT AKKARAEKTHALIN (Member, IEEE) received the B.Eng. and M.Eng. degrees in electrical engineering from the King Mongkut's University of Technology North Bangkok (KMUTNB), Bangkok, Thailand, in 1986 and 1990, respectively, and the Ph.D. degree from the University of Delaware, Newark, DE, USA, in 1998.

From 1986 to 1988, he was a Research and Development Engineer with Microtek Products Company Ltd., Thailand. In 1988, he joined the Department of Electrical Engineering, KMUTNB. He was the Head of the Senior Research Scholar Project, which is supported by the Thailand Research Fund, from 2015 to 2017. He has authored or coauthored more than 40 international journals, 200 conference papers, and four books/book chapters. His current research interests include RF/microwave circuits, wideband and multiband antennas, telecommunication, and sensor systems.

Dr. Akkaraekthalin is a member of the Institute of Electronics, Information and Communication Engineers (IEICE), Japan, the Electrical Engineering/Electronics, Computer, Telecommunications, and Information Technology (ECTI), and the Electrical Engineering Academic Association (EEAAT), Thailand. He was the Chairperson of the IEEE Microwave Theory and Techniques/Antennas and Propagation/Electron Devices (MTT/AP/ED) Thailand Joint Chapter, from 2007 to 2010, and the Vice President and the President of the ECTI Association, Thailand, from 2012 to 2013, and from 2014 to 2015, respectively. He was the Editor-in-Chief of the *ECTI Transactions*, from 2011 to 2013.

NUTAPONG SOMJIT (Senior Member, IEEE) received the Dipl.-Ing. (M.Sc.) degree from the Dresden University of Technology, Dresden, Germany, in 2005, and the Ph.D. degree from the KTH Royal Institute of Technology, Stockholm, Sweden, in 2012.

Then, he returned to TU Dresden to lead a research team in microsensors and MEMS ICs for the Chair for Circuit Design and Network Theory. In 2013, he was appointed as a Lecturer (an Assistant Professor) with the School of Electronic and Electrical Engineering, University of Leeds, Leeds, U.K., where he is currently an Associate Professor. Since 2022, he has been appointed to lead a research team as an Adjunct Faculty Member of the Micro and Nanosystems Department, KTH Royal Institute of Technology. His research interests include integrated smart high-frequency components, sustainable micro and nanosystems, and low-cost microfabrication processes.

Dr Somjit was appointed as a member of the Engineering, Physical and Space Science Research Panel of the British Council, in 2014. He was a recipient of the Best Paper Award (EuMIC Prize) at the European Microwave Week, in 2009. He was awarded the Graduate Fellowship from the IEEE Microwave Theory and Techniques Society (MTT-S), in 2010 and 2011, and the IEEE Doctoral Research Award from the IEEE Antennas and Propagation Society, in 2012. In 2016, he was the Chair of the Student Design Competition for the European Microwave Week, and in 2018, he was appointed as an Associate Editor of *Electronics Letters* (IET).